



Deposited via The University of Sheffield.

White Rose Research Online URL for this paper:

<https://eprints.whiterose.ac.uk/id/eprint/196496/>

Version: Published Version

Article:

Scullion, E., Morgan, H., Lin, H. et al. (2022) SULIS: a coronal magnetism explorer for ESA's Voyage 2050. *Experimental Astronomy*, 54 (2-3). pp. 317-334. ISSN: 0922-6435

<https://doi.org/10.1007/s10686-022-09877-2>

Reuse

This article is distributed under the terms of the Creative Commons Attribution (CC BY) licence. This licence allows you to distribute, remix, tweak, and build upon the work, even commercially, as long as you credit the authors for the original work. More information and the full terms of the licence here:

<https://creativecommons.org/licenses/>

Takedown

If you consider content in White Rose Research Online to be in breach of UK law, please notify us by emailing eprints@whiterose.ac.uk including the URL of the record and the reason for the withdrawal request.



SULIS: A coronal magnetism explorer for ESA's Voyage 2050

E. Scullion¹ · H. Morgan² · H. Lin³ · V. Fedun⁴ · R. Morton¹

Received: 30 July 2020 / Accepted: 17 October 2022
© The Author(s) 2022

Abstract

Magnetism dominates the structure and dynamics of the solar corona. To understand the true nature of the solar corona and the long-standing coronal heating problem requires measuring the vector magnetic field of the corona at a sufficiently high resolution (spatially and temporally) across a large Field-of-View (FOV). Despite the importance of the magnetic field in the physics of the corona and despite the tremendous progress made recently in the remote sensing of solar magnetic fields, reliable measurements of the coronal magnetic field strength and orientation do not exist. This is largely due to the weakness of coronal magnetic fields, previously estimated to be on the order of 1-10 G, and the difficulty associated with observing the extremely faint solar corona emission. With the Solar cUbesats for Linked Imaging Spectro-polarimetry (SULIS) mission, we plan to finally observe, in detail and over the long-term, uninterrupted measurements of the coronal magnetic vector field using a new and very affordable instrument design concept. This will be profoundly important in the study of local atmospheric coronal heating processes, as well as in measuring the nature of magnetic clouds, in particular, within geoeffective Earth-bound Coronal Mass Ejections (CMEs) for more accurate forecasting of severe space weather activity.

Keywords Sun · Telescopes

✉ E. Scullion
eamon.scullion@northumbria.ac.uk

¹ Northumbria University, NE1 8ST Newcastle upon Tyne, UK

² Department of Physics, Aberystwyth University, SY23 3BZ, Cymru, Ceredigion, UK

³ Institute for Astronomy, University of Hawai'i, 96768, HI, Pukalani, USA

⁴ Department of Automatic Control and Systems Engineering, University of Sheffield, Sheffield, UK

1 Introduction

Coronal physics has progressed enormously over the last decade with the advent of new observations from ground- and space-based instruments. However, many critical questions regarding the structure, heating, and dynamics of the corona will remain open until we can reliably and routinely measure the properties of coronal magnetic fields. Most solar activity, including high-energy electromagnetic radiation, solar energetic particles, flares, and coronal mass ejections, derives its energy from coronal magnetic fields. The corona is also the source of the solar wind with its embedded magnetic field that engulfs the Earth. These phenomena are collectively responsible for perturbations on the Earth's environment, known as space weather, that affect communications, space flight, and power transmission. Measuring magnetic fields in the solar corona is a necessary step towards understanding and predicting the Sun's generation of space weather.

Direct measurement of the magnetic fields in the corona is very difficult, and past results are inconclusive because of large uncertainties. For example, the strongest field detected by early magnetograph observations of the Zeeman effect in the green Fe XIV coronal emission line (CEL) was 13 ± 20 G [10]. Linear polarisation measurements of the Hanle effect in CELs have been more effective in measuring the CEL linear polarisation in the visible and near-IR wavelengths. The saturated Hanle effect is due to resonant scattering of photospheric radiation by highly ionised atoms in the solar corona. This relies on the assumptions of an optically thin atmosphere, anisotropic illumination, and low collisional rates, as demonstrated in the cartoon of Fig. 1.

CEL linear polarisation yields information about the orientation of coronal magnetic field vectors projected in the plane of the sky, subject to the Van Vleck effect, and there can be substantial linear polarisation signals of 1-10%. They were first measured in the 1960s and 1970s and today routine full-corona ($< 1.4 R_{Sun}$) observations are performed with the High Altitude Observatory Coronal Multi-channel Polarimeter (CoMP: [34]) instrument. Linear polarisation measurements of the Hanle effect in CELs have been more successful in mapping the direction of coronal magnetic field vectors in the plane-of-sky [2, 21, 26], however, these measurements are not sensitive to the strength of the magnetic field [3, 17]. CEL circular polarisation (CP) signals, which are proportional to the strength of the line-of-sight (LOS) component of the magnetic field, are very weak with amplitudes of 0.1% of the line intensity or lower [18, 19]. The first spectroscopic measurements of a CEL polarisation signal above an active region in the solar corona is presented in Fig. 2, as reported in [19].

More recently, CoMP measured a noise level of a few Gauss and this was achieved with 4.5 arcsecond pixels in 2.4 hours of integration using a 20 cm aperture coronagraph. Given that we are photon noise limited, the performance demonstrated here can only be improved with more photons. In order to address this, the next generation (COSMO: [35]) ground-based facility (successor to CoMP) will lead to the construction of larger solar coronagraphs (1.5 m aperture) for ensuring better signal-to-noise in the polarimetric accuracy to acquire

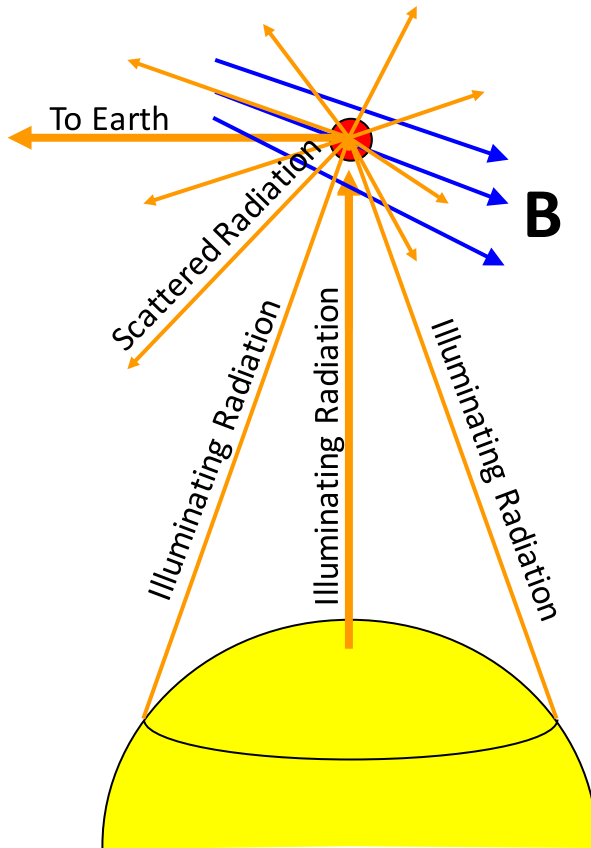


Fig. 1 Conceptual description of the saturated Hanle Effect, whereby the yellow sphere represents the Sun, the orange lines represent the photospheric radiation emanating from the Sun surface, the blue lines are the magnetic field lines in the corona and the red circle is an ionised atom scattering the photospheric radiation

sufficient measurements of Stokes V and the circular polarisation for magnetic field strengths with a necessary reduction in the effective integration time for the measurement. Similarly, the Diffraction-Limited Near-Infrared Spectro-polarimeter (DL-NIRSP) on the 4-m Daniel K. Inouye Solar Telescope (DKIST: [11]) will perform a similar measurement of the coronal magnetic field over a small FOV (limited to mosaicking of $\sim 21 \times 14''$ mosaic tiles). While the completion of DKIST will enable more routine measurements of CEL circular polarisation, these observations will be limited to a small field of view (FOV) in the low corona.

This LOS integration makes it impossible to directly derive the instantaneous magnetic field ($\mathbf{B}(\mathbf{r};t)$), temperature ($T(\mathbf{r};t)$), and density ($n(\mathbf{r};t)$) from spectra observed from a single view-point, except in cases such as bright loops when it can be assumed that the emission originates from a localized source. This has been a fundamental limitation of ground-based coronal observations. Nevertheless,

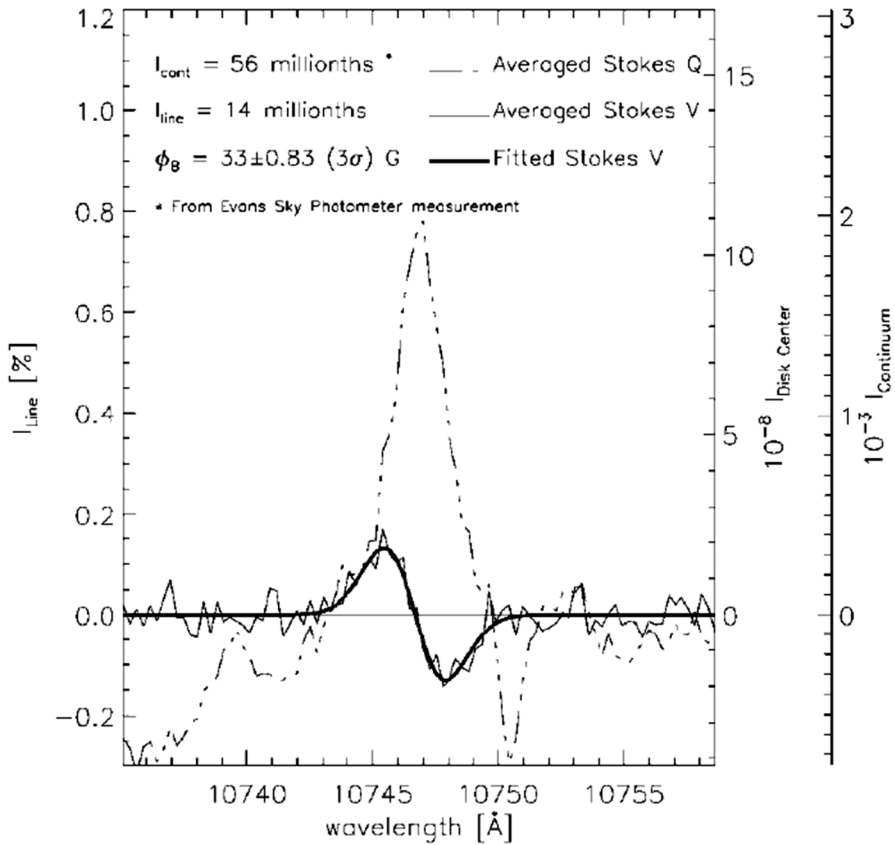


Fig. 2 Stokes Q and V profiles averaged over the entire FOV for the observations reported in [19]. The magnetic antisymmetric profile of the Stokes V spectrum is clearly shown. The calibration to disc-centre intensity was obtained from a sky brightness measurement using the National Solar Observatory (NSO) Evans Sky Photometer

scalar and vector tomographic inversion techniques have been successfully developed in order to disentangle the 3D structure of the coronal magnetic field. Such tomographic inversion tools are tailored to existing observing capabilities [12] and applied to CoMP linear polarisation data. Although this is a major step forward in our quest for direct observational inference of $\mathbf{B}(\mathbf{r};t)$, its accuracy and applicability are still subject to the limitations of existing instrumentation. For example, tomography with only linear polarisation measurements is insensitive to certain magnetic field configurations [12]. Therefore, more effort is needed to develop a tomographic inversion code that incorporates both the linear and circular polarisation signals of multiple CELs.

Furthermore, detecting and tracking CME eruptions and measuring the properties of the magnetic cloud of a CME will require continuous monitoring of the global corona, and to understand the nature of the corona will require synoptic

measurements without interruption and with multiple viewing angles to avoid the limiting Van Vleck effect and 180 degree ambiguity in measuring transverse magnetic field components. Therefore there is a need to place multiple, spectro-polarimetric instruments like CoMP in space to ensure long-term uninterrupted measurements, utilising the collective power of stereoscopy, at an affordable cost. Furthermore, we need to further reduce the integration times while retaining a large FOV to track evolution in the fast evolving CMEs. That is the motivation behind this low cost, technology demonstration space-mission concept to be outlined next.

2 Science objectives

2.1 Coronal atmospheric diagnostics

The goals of understanding the physical mechanisms behind coronal plasma heating and solar wind acceleration are still pertinent. This is due to the potential for different mechanisms, e.g., waves dissipation, turbulence, magnetic reconnection, and instabilities, to contribute by varying amounts to the energy flux of geometrically distinct magnetic regions (i.e., active regions, closed quiescent loops, open field lines). Recent interest in the forecasting of space weather has added a fresh impetus for making progress in these problems of heating and wind acceleration. In particular, the ability to make predictions of both slow and fast solar wind stream properties, and to understand their variability, are key aspects for determining particle fluxes into the near-Earth environment and are a contributor to the evolving kinematics of coronal mass ejections through the heliosphere.

Recently, a potential basal contribution to the energy budget has been identified in imaging and spectroscopic observations and interpreted in terms of Alfvénic wave energy [20, 31, 33]. Alfvénic waves have long been assumed to play a significant role in heating plasma, their incompressible nature enabling them to transfer energy over large distances. CoMP was the first instrument to provide evidence for the Alfvénic wave energy flux through the solar atmosphere [33], and subsequent investigation has revealed the ubiquity and persistence of this wave flux in Doppler velocities [23, 24, 32].

These observations have come in conjunction with some success in producing a heating of coronal plasma from wave-driven turbulence models [6, 9, 30], along with reproducing some of the basic properties of slow and fast solar wind. However, there are a number of challenges that these models have to overcome [5, 25], requiring more stringent observational constraints on the mechanisms for delivering energy, mass, and momentum in the source regions in the low corona. Moreover, current forecasting models employ empirical techniques that have provided relative levels of success, although they are limited in their predictive power due to the neglect of the physical mechanisms ultimately responsible for plasma heating and wind acceleration. For example, the Wang, Sheeley & Arge (WSA) model [1, 38], relies upon a static, potential coronal field and an empirical formula to estimate wind speed, while the Magnetohydrodynamics-Around-a-Sphere (MAS) model [22] generates a wind by adding an ad-hoc heating function. Success in advancing knowledge of

the underlying physics and improving forecasting will depend on determining the energy, momentum, and mass flux through different magnetic regions, quantifying the relative contributions of the plethora of potential mechanisms, and detailed knowledge of the free energy in the coronal magnetic field.

Initial results from CoMP have shown promise for synoptic Doppler imaging of the extended corona to contribute to our understanding of the coronal magnetic field and Alfvénic energy flux through the solar atmosphere, with the potential to constrain key features of both sets of models. Recent CoMP results demonstrate the capability to make unique insights into wave phenomenon, e.g., wave excitation and damping/mode conversion; Alfvénic turbulence; relative energy fluxes through distinct regions of the corona; energy flux from the lower solar atmosphere to the solar wind [7, 23, 24, 32, 37]. Additionally, CoMP has demonstrated such instruments have the potential for the exploitation of waves through magneto-seismology, in combination with spectroscopic techniques, to determine local plasma conditions, e.g., measurements of the magnetic field and relative angle with respect to the solar surface. Further, this combination can also provide estimates of the outflow of plasma low in the corona [23], allowing constraints to be placed on mass and energy flux along open-field lines and from regions potentially contributing to the slow solar wind.

Further science questions to be explored include:

- i) What are the key physical mechanisms contributing to coronal heating in different magnetic geometries?
- ii) What is the relative wave energy flux through different magnetic regions?
- iii) Are the waves able to deposit their energy in the solar corona? And what are the physical rates for energy deposition?
- iv) Is there evidence for the development of Alfvén wave turbulence in the lower corona?
- v) What is the role of waves in the acceleration of the solar wind?
- vi) What is the evolution of these waves in outer layers of the solar atmosphere, between the solar corona and the solar wind?
- vii) How does the wave energy flux vary over the course of the solar cycle?
- viii) Which regions are key contributors to solar wind streams?
- ix) Is it feasible to exploit MHD waves via magneto-seismology to provide routine and meaningful characterisation of the plasma and magnetic field conditions in the corona?

2.2 Magnetic fields in solar eruptions

Observational determination of the 3D magnetic and thermodynamic structure of the solar atmosphere requires measurements of magnetic field configuration and thermodynamic conditions of the solar plasma in a) the photosphere, b) the chromosphere, and c) the corona above. Observations of photospheric magnetic fields are well established [13], and current instruments such as the Helioseismic and Magnetic Imager (HMI) of the Solar Dynamic Observatory (SDO) and the

Spectro-Polarimeter (SP) of the Hinode Mission provide routine and high-quality data for photospheric vector magnetic fields. While many ground-based instruments can measure chromospheric magnetic fields, none can measure them with all the performance required for the study of energetic solar eruptions.

Coronal mass ejections (CMEs) consist of large structures containing plasma and magnetic fields that are expelled from the Sun into the heliosphere. CMEs are a key aspect of coronal and interplanetary dynamics. They inject large quantities of mass and magnetic flux into the heliosphere, causing major transient disturbances at Earth. White-light CME observations mainly provide information on the mass content of the CME but very little on the magnetic structure. They are thought to remove built-up magnetic energy and plasma from the solar corona and most of the ejected material comes from the low corona. However, cooler, dense material of chromospheric or photospheric origin is sometimes involved. The CME plasma is entrained on an expanding magnetic field exhibiting helical field lines with changing pitch angles, commonly referred to, as a flux rope. The onset of CMEs has been associated with many solar disc phenomena such as flares, prominence eruptions, coronal dimming, arcade formation, X-ray sigmoids, and both thermal and non-thermal CME radio emission in the form of shocks. However, the vast majority of the ejected energy assumes the form of mechanical energy carried by the CME and not the associated solar flare, even in the most energetic cases. CMEs can exhibit a variety of forms with some having the classical “three-part” usually interpreted as compressed plasma ahead of a flux rope followed by a cavity surrounded by a bright filament or prominence. Other CMEs display a more complex geometry and appear as narrow jets. Some arise from pre-existing coronal streamers (streamer blowouts), while others appear as wide, almost global, eruptions such as Halo CMEs. Their speeds, accelerations, masses, and energies extend over 2-3 orders of magnitude and their angular widths exceed by factors of 3-10 the sizes of flaring active regions. Many CMEs have also been observed to be unassociated with any obvious solar surface origin and most flares occur independently of CME eruptions, it now seeming likely that any flare accompanying a CME is part of an underlying magnetic process rather than being a direct cause of the CME [39]. Recent models describing the onset and early evolution of CMEs provide a variety of mechanisms behind their formation. More significantly, CMEs can drive interplanetary shocks which are a key source of solar energetic particles and they are known to be the major contributor to severe space weather at the Earth (i.e. they are geoeffective).

Energetic CME eruptions, micro-flares, impulsive flares, and long-duration flares can exhibit spatial scales ranging from 5 Mm to 400 Mm and temporal scales ranging from 60 s to 10^5 s, yet, these may all be manifestations of the same underlying magnetic reconnection process [27]. On the other hand, large-scale coronal magnetic structures above flare sites may have direct influence on whether coronal mass ejections occur with flares [29]. Therefore, a thorough understanding of the physics of solar eruptions requires observations of the magnetic and plasma interactions in a large 3D volume of the solar atmosphere before, during, and after the eruptions with a high cadence and resolution sufficient to resolve the dynamic time scale and spatial scale of solar eruptions.

Further science questions to be addressed in relation to magnetic field measurements of CME's include:

1. What triggers the release of free energy in closed magnetic fields leading to CME initiation?
2. Are there two physically different processes that launch CMEs (i.e. one for flare-driven and one for prominence eruptions) or do all CMEs belong to a dynamical continuum with a single physical initiation process?
3. How is the free energy apportioned between the flare energy and the CME mechanical energy?
4. How significant are pre-eruption minor energy releases as a true precursor to a CME? Or are they only separate eruptions?
5. Can we better quantify the propelling and retarding forces that impact upon CMEs, in the corona and interplanetary medium, in order to more accurately predict the arrival at Earth?
6. Why do the fastest CMEs and seemingly more energetic events produce only low levels of solar energetic particles (SEPs)?
7. Do magnetic clouds exist within CMEs in the corona and what are their magnetic properties? Do they all consist of a flux rope structure?
8. Is there any relationship between magnetic complexity in a source region and CME productivity?
9. Does the magnetic cloud structure of a CME have a definite leading and trailing field orientation? Can we accurately forecast how geoeffective a CME in the corona will become?

3 SULIS mission concept

Here we propose a mission concept called Solar cUbeSats for Linked Imaging Spectro-polarimetry (SULIS¹). SULIS consists of formation-flying CubeSat pairs that provide very high (eclipse-like) quality observations of the solar atmosphere. SULIS will lead a step-change in human understanding of the key physics that governs the nature of the Sun-Earth environment, through innovative 10U CubeSat technology. A critical technology within the mission design, is inter-satellite laser communications for enabling high speed data transfer between the satellites and the ground and for maintaining formation flying and solar disc occultation. To date, the SULIS project has received £1M in funding from UK Space Agency (UKSA) to design, build and test a novel laser communications terminal applicable to small satellites (specifically CubeSats) to serve as a technology demonstrator for SULIS. SULIS will place three pairs of formation-flying coronagraphs within CubeSats in 1AU orbits around the Sun. The sunward occulting CubeSat of each pair will observe the solar disc and, uniquely, act as an external occulter for the anti-sunward coronagraph CubeSat, which will observe the extended corona, as depicted in the upper panel of Fig. 3.

¹ <http://sulis.space>

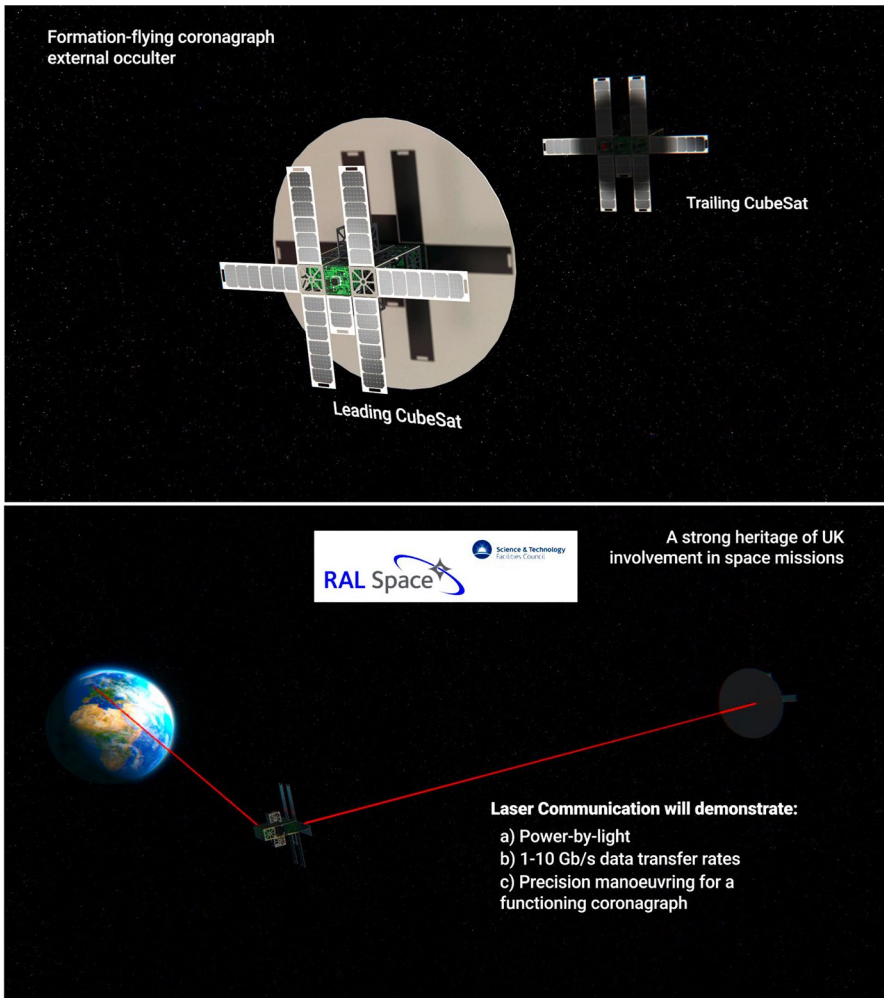


Fig. 3 *Top:* A 90 cm diameter external occulter extends (post-launch) from the sunward Leading CubeSat, resulting in an artificial eclipse falling on the anti-sunward Trailing CubeSat instrumentation, with a separation of 100 m. The pair of CubeSats will fly in formation maintaining positioning via an ion propulsion thruster system throughout the 5-year mission lifetime. Uniquely, the Leading CubeSat serves as an occulter, as well as housing instrumentation for solar observations. *Bottom:* A key aspect of the SULIS mission will be the technology demonstration of Li-Fi, which has the potential to revolutionise satellite-to-satellite and satellite-to-ground communications

Each CubeSat pair will fly in formation, the first pair in Earth orbit and the other two pairs drifting away, ahead of and behind Earth in its orbit, for a mission lifetime of 5-10 years.

The overall aim of SULIS is to understand the Sun’s link to the inner heliosphere via revolutionary UK-led technology. For international relevance, SULIS will provide unprecedented measurements of the magnetic field of the corona answering

fundamental questions that underpin the sources of space weather. This aligns perfectly with the UK Space Innovation and Growth Strategy². SULIS offers bespoke technology demonstration testing smart CubeSat optical communication, multi-purpose radiation-hardened PhotoVoltaic (PV) cells invoking power-by-light technology, via visible light communications known as Li-Fi, depicted in the lower panel of Fig. 3.

Despite the hazards of space weather to terrestrial infrastructure (UK National Risk Register for Civil Emergencies³, 2020), routine monitoring of space weather is limited to two ageing scientific missions (SOHO and STEREO; RAL space scientists are Principal Investigators on both of these missions).

3.1 SULIS key objectives

The three key objectives of SULIS are:

- 1) Provide the first direct measurements of the 3D coronal magnetic field.
- 2) Provide eclipse-quality imaging of the extended solar corona (out to $5 R_{Sun}$) for deeper understanding of fundamental science underpinning space weather.
- 3) Demonstrate UK-led future technologies (i.e. smart CubeSats; radiation-hardened solar cells; laser optical communications: Li-Fi).

SULIS will capitalise on the diagnostic properties of coronal forbidden emission lines in the visible/near-IR, to determine the 3D vector magnetic field routinely, and to measure electron temperatures, ion densities, elemental abundances, charge states, bulk flow speeds, and non-thermal heating (i.e. wave heating). Observations of forbidden coronal emission lines in the visible/near-IR have been neglected in current solar missions. The region from the base of the corona out to a height of $3 R_{Sun}$ is important – it is where Coronal Mass Ejections (CMEs) and the solar wind are formed and accelerated. Yet there are no routine quality measurements of this region: there are no direct measurements of the coronal magnetic field, and no quality measurements of the plasma properties. Through multiple CubeSats, the SULIS mission⁴ will directly address this missing link. SULIS will complement operational space weather missions, for e.g. ESA's potential Vigil mission (previously known as L5 or Lagrange), PROBA-3 mission (ESA's follow-on to the NOAA's DSCOVR), and pave the way for future technology demonstrations, such as the ESA-DOCS⁵[28] and INSTANT⁶[14] mission concepts.

Three pairs of CubeSats will fly in formation: the first pair in Earth polar orbit and the other two pairs drifting ahead of and behind Earth in a 1AU orbit. The sunward CubeSat of each pair will act as an external occulter for the other CubeSat,

² https://www.ukspace.org/wp-content/uploads/2020/04/Space-IGS-Main-Report_Feb2010.pdf

³ <https://www.gov.uk/government/publications/national-risk-register-2020>

⁴ <http://sulis.space>

⁵ <https://ieeexplore.ieee.org/document/8357207/>

⁶ <https://instantmission.wordpress.com/>

which will observe the corona. This unique configuration provides eclipse-quality observation, and the three widely-separated viewpoints allows 3D reconstruction of the coronal magnetic field, plasma, and CMEs.

3.2 Instrument 1: Coronagraph

The SULIS payload consists of a coronagraphic high-resolution multichannel spectrometer together with a state-of-the-art broadband hyperspectral imager for observing the off-disc extended corona. The high-resolution spectrometer element of this instrument has been developed through an STFC PRD grant (ST/N002962/1 2016–19). An accompanying novel hyperspectral imager is included, linked to the development of the PanCam instrument [4] on ExoMars. This novel hyper-spectral design includes a linear variable filter in front of a detector that provides a 2D image which varies in wavelength along one axis, scanning the camera across the target builds up the hyperspectral data cube. The SULIS imaging system is simpler and more compact than conventional pushbroom hyperspectral imagers. The visible coronagraph will be hosted on the anti-sunward coronagraph CubeSat of each pair. The proposed instrument will simultaneously collect high-resolution spectral data of several coronal emission lines along a spatial slit, which will scan across the corona. No other space- or ground-based mission will routinely collect data of this clarity in the range of $1.5\text{--}3 R_{Sun}$ from the Sun.

3.3 Instrument 2: Spectropolarimeter

Magnetic fields shape the temperature and density structure of the corona and underpin all dynamic eruptions such as flares and CMEs. The energy released in dynamic eruptions is stored in the coronal magnetic field. Measurements of the surface magnetic field have limited utility for space weather forecasting, therefore, precise knowledge of the 3D properties of the coronal magnetic field is critical. The SULIS spectropolarimeter consists of a 99-slit, massively-multiplexed coronal spectro-polarimeter for measuring the low-corona 3D magnetic field. The spectropolarimeter enables determination of magnetic fields, temperatures, and densities from emission line polarisation. Inversion of the Fe *XIII* $1.075 \mu\text{m}$ and He *I* $1.083 \mu\text{m}$ spectra give magnetic fields through the saturated Hanle effect. Current telescopes and instruments can only measure the coronal magnetic field strength over a small field of view. Furthermore, the observations require very long integration times that preclude the study of dynamic events even when only a small field of view is required. A new instrument concept that employs large-scale multiplexing technology to enhance the efficiency of current coronal spectropolarimeters by more than two orders of magnitude is outlined in [16]. This will allow for the instrument to increase the integration time at each spatial location by the same factor, while also achieving a large field of view coverage. The 99-slit coronal spectropolarimeter can observe six coronal emission lines simultaneously. Instruments based on this concept will allow us to study the evolution of the coronal magnetic field even with coronagraphs with

Table 1 Estimates of the spectro-polarimeter signal-to-noise ratio and detectability of the Fe XIII 1.075 μm line, as reported by [16]

Observing Mode	$\Delta x \times \Delta y$	Δt	T_{map}	I_{SC}	SN_I	SN_L	SN_V	$B_{3\sigma}$
1. Full-field scan	1'' \times 1''	1.5s	1m	5	256	13	0.26	117G
1a. 20'' average of Mode 1	20'' \times 20''	1.5s	1m	5	5120	256	5	6G
1b. 10 min average of 1a	20'' \times 20''	15s	10m	5	16250	810	16	2G
2. Sit-and-Stare mode	1'' \times 1''	5m	5m	5	3600	180	4	8G
3. Full-field Scan	1'' \times 1''	1.5s	1m	0.5	810	40	0.8	37G
3a. 10'' average of Mode 3	10'' \times 10''	1.5s	1m	0.5	8100	400	8	4G

modest aperture. The proof-of-concept instrument, *mxSPEC*, was assembled at the full-disc port of the Dunn Solar Telescope (DST) in 2014 using DST inventory optics, a He I 1083 nm DWDM bandpass isolation filter (BIF) with 1.4 nm bandpass, and a 10 frames per second (fps) IR camera [15]. Table 1 presents a short summary of the potential instrument capabilities based upon a similar *mxSPEC* design.

The most important aspect of a coronagraph design is the scattered light performance of the optical system. With the simple optical system the instrument will have very high photon throughput. Using a circular polarisation amplitude of 1×10^3 for a 10 G magnetic field, the estimated 3σ detection limits of the line-of-sight component of the coronal magnetic field or the Fe XIII 1.075 μm line are 35 G, 12 G, and 4 G, respectively, with spatial resolution of 1'', 3'', and 10'', and temporal resolution of 2 hours per map if the scattered light background is kept sufficiently low. Super-polishing technology for fabrication of a new coronagraph objective lens (preferable to mirrors with regard to minimising scattering) with 0.01 ppm scattered light is now feasible. Such technological advances mean that the fabrication of ultra-low scattered light optics with high-grade fiber-optic glass enabling low internal scattering of 0.1 nm RMS is achievable. This is sufficient to measure the coronal magnetic field in most active regions up to $1.4 R_{Sun}$. For comparison, it would take a conventional single slit spectro-polarimeter a minimum of 26.7 hours of observation to obtain one full-polarisation map of the 1.2×1.0 degree field. Furthermore, multi-slit, multi-spectral spectrographs increase system throughput of individual telescopes by a factor of 500, and will enable multi-temperature and density measurements for a large FOV far off-limb (Table 2).

A perspective combined FOV for SULIS, incorporating the leading instrumentation capturing on-disc solar observations and the trailing instrumentation capturing far off-limb solar observations is shown in Fig. 4. Utilising simultaneous observations from the other CubeSats enables tomographic inversions of spectral lines, thus gaining a 3D mapping of the field and plasma structure. Clusters of small ~ 10 cm telescopes (suitable for CubeSats) operating collectively can achieve the same magnetic field sensitivity as a large ~ 1 m telescope, but at a significant cost saving.

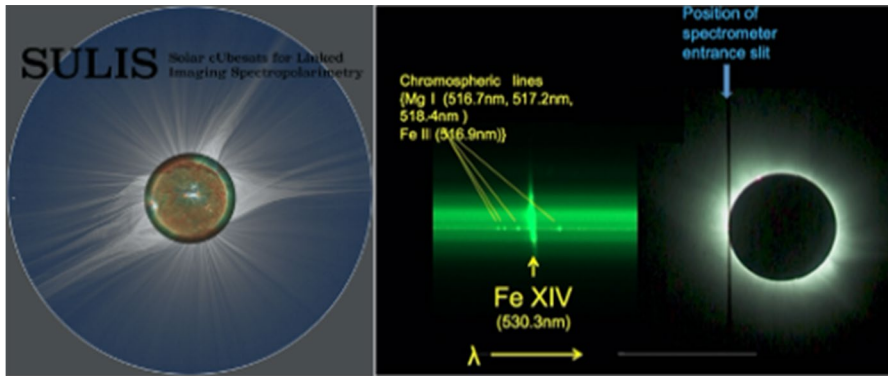


Fig. 4 *Left:* The spectro-polarimeter (occluding CubeSat) will observe the solar disc and inner atmosphere. The coronagraph (coronagraph CubeSat) will observe extended coronal structures and CMEs. *Right:* Example of the spectrometer eclipse measurements. The slitjaw image on the right shows the slit position, the high-resolution spectra are on the left

Table 2 Estimates of mxCSM Signal-to-Noise ratio and detectability of the Fe XIII 1.075nm line

Observing Mode	$\Delta x \times \Delta y$	Δt	T_{map}	I_{sc}	SN_I	SN_L	SN_V	$B_{3\sigma}$
1. Full-field scan	1'' × 1''	1.5s	1m	5	256	13	0.26	117G
1a. 20'' average of Mode 1	20'' × 20''	1.5s	1m	5	5120	256	5	6G
1b. 10 min average of 1a	20'' × 20''	15s	10m	5	16250	810	16	2G
2. Sit-and-Stare mode	1'' × 1''	5m	5m	5	3600	180	4	8G
3. Full-field Scan	1'' × 1''	1.5s	1m	0.5	810	40	0.8	37G
3a. 10'' average of Mode 3	10'' × 10''	1.5s	1m	0.5	8100	400	8	4G

3.4 Important Advances in Technology for the Future

There is no bigger question in solar physics than “What is the origin of coronal heating?” Measuring magnetic vector fields of the global solar corona via coronagraphs will give us the necessary insight into the nature of coronal heating. The SULIS mission aims to do exactly that.

The mission is of particular importance because there currently is no plan to have a space-based coronagraph as a follow-up to full-disc, uninterrupted synoptic studies of CME’s. The measurement of the geoeffectiveness of eruptions leading to space weather is becoming increasingly important given our increasing reliance on satellite communications. To understand the geoeffective nature of CMEs with enough warning requires measuring the magnetic field of CMEs close to the source rather than near Earth via in-situ measurements.

The use of CubeSats for an ambitious space mission sets a benchmark for future cost-effective missions. The technological innovations of SULIS will advance power efficiency, communications, and control for CubeSats and constellations,

with impact on future space applications, and will address the central problem of CubeSat clusters, i.e. formation flying control, scientific instrumentation integration, and a novel laser optical communications demonstration for data transfer. Precision maneuvering is of substantial interest within the international spaceflight community, e.g., the AAREST⁷ mission. Therefore, SULIS has the potential to strengthen the collaborative relationship between the UK's Science and Technology Facilities Council (STFC) and the space industry who build ESA's missions.

SULIS will see the application of laser optical communications in space. VLC offers a wide range of applications including short range optical wireless networks for healthcare, medium range inter-vehicular and vehicle-to-infrastructure communications [36].

In terms of the potential for societal and economic impact, SULIS will enable us to better understand the drivers of space weather. The cost of space weather impact is enormous [8]: The failure of the Hydro-Quebec system in 1989 during a solar storm took 9 hours to restore 80% of operations leaving 5 million people without power and costing Can\$ 2 billion in economic losses. The definitive extreme space weather scenario is the famous 1859 Carrington event. Lloyd's of London⁸ estimated the cost of a similar event today would be £1-2 trillion, based on calculations examining disruption to the global supply chain.

The UK government *Space Weather Preparedness Strategy*⁹ (2015) describes the risk to the UK from severe space weather, prepared by the UK Department for Business, Energy & Industrial Strategy (BEIS). Government departments must plan for this risk across society, including military, energy, civil aviation, and transport in general. A variety of impacts are presented in Fig. 5. SULIS will provide important data to inform many policy-enforcing agencies and future large-scale infrastructure planning by the UK and European governments.

3.5 Timeliness

Placing SULIS CubeSats housing instruments at multiple locations in Earth's orbital path, i.e. one in a Sun synchronous orbit and one at Lagrangian point L5 has the following advantages:

1. A multi-FOV perspective (via instrument #1 (Coronagraph) and #2 (Spectropolarimeter)) of CME eruptions will enable tracking from the coronal mode (#1) FOV to a wider field interplanetary mode (#2).
2. The multiple viewpoints will directly address the 180 degree ambiguity in the linear polarisation measurement.
3. The instruments can combine data to measure the circular polarisation (Stokes V) and magnetic field strength of the same source or CME twice as fast.

⁷ <https://directory.eoportal.org/web/eoportal/satellite-missions/a/aarest>

⁸ Lloyd's. Solar storm risk to the North American electric grid. London UK: Lloyd's, 2013. Available at: <https://www.lloyds.com/news-and-insights/risk-reports/library/solar-storm>

⁹ <https://www.gov.uk/government/publications/space-weather-preparedness-strategy>

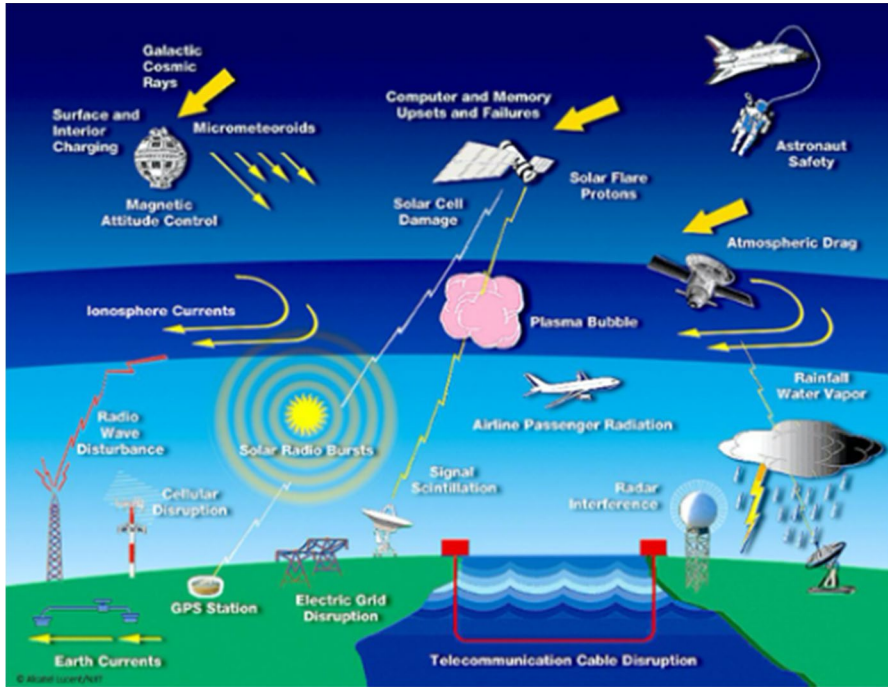


Fig.5 Modern society is increasingly at risk from many space weather impacts (image credit: Alctel/ NJIT)

4. Placing the instrument in space reduces the scattering of the polarisation signal which has limited measurements of the weak fields from the ground, thereby ensuring further reductions in the integration time.

3.6 Summary

We have described a concept for a new instrument, optimized for high-temporal resolution spectroscopic measurements of the intensity and polarisation of multiple CELs over a very large field of view for research in coronal magnetism. For comparison, the time required for the 25 cm aperture, 6-line, 99-slit coronal spectropolarimeter coronagraph presented in this paper to observe the 1 degree FOV is comparable to that of a 6-m coronagraph equipped with current single-slit, single-wavelength spectro-polarimeter. SULIS can be constructed with only a fraction of the cost required for the construction of a 6-m class coronagraph. The high system throughput of this design also makes it an ideal design for future space missions where size and weight of the instruments are severely limited.

Acknowledgements We are grateful to the members of the Proposing Team for their contributions to the SULIS mission: Dr Jackie Davies, Heliospheric Team Leader, STFC RAL Space (UK); Philip Steen, Head of Technology, Andor Technology Ltd (UK); Mark Gibbs, Head of Space Weather, UK Met Office (UK); Prof Shadia Habbal, IfA, University of Hawaii (USA); Prof Adalbert Ding, Technische Universitaet Berlin (Germany); Prof Stuart Irvine, Centre for Solar Energy Research (CSER), Swansea University

(UK); Dr Dan Lamb, CSER, Swansea University (UK); Dr Matt Gunn, Aberystwyth University (UK); Prof James McLaughlin, Northumbria University (UK); Dr Shaun Bloomfield, Northumbria University (UK); Dr Patrick Antolin, Northumbria University (UK); Dr Neil Beattie, Northumbria University PhotoVoltaics (NUPV), Northumbria University (UK); Prof Z. Ghassemlooy, Optical Communications Research Group (OCRG), Northumbria (UK); Prof Mihalis Mathioudakis, Queens University Belfast (QUB) (UK); Prof Gerry Doyle, Armagh Observatory and Planetarium, (UK); Prof Sarah Mathews, Mullard Space Science Laboratory, University College London (UK); Prof Robertus von Fay-Siebenburgen, University of Sheffield (UK); Dr Viktor Fedun, University of Sheffield (UK); Dr. A.K. Srivastava Indian Institute of Technology (India); Dr Kostas Tziotziou National Observatory of Athens (Greece); Dr Georgia Tsiropoula National Observatory of Athens (Greece); Dr David Pontin University of Dundee (UK); Prof Valery Nakariakov, University of Warwick (UK); Dr Istvan Ballai University of Sheffield (UK); Dr Gary Verth, University of Sheffield (UK); Dr Peter Keys, Queens University Belfast (UK); Prof Lucie Green, Mullard Space Science Laboratory, University College London (UK); Dr Mathew Owens, University of Reading (UK); Prof Peter Gallagher, Trinity College Dublin (Republic of Ireland)

Data Availability All data presented in this manuscript will be made available upon request to the corresponding author.

Declarations

Conflicts of interest All authors declare that they have no conflicts of interest.

Open Access This article is licensed under a Creative Commons Attribution 4.0 International License, which permits use, sharing, adaptation, distribution and reproduction in any medium or format, as long as you give appropriate credit to the original author(s) and the source, provide a link to the Creative Commons licence, and indicate if changes were made. The images or other third party material in this article are included in the article's Creative Commons licence, unless indicated otherwise in a credit line to the material. If material is not included in the article's Creative Commons licence and your intended use is not permitted by statutory regulation or exceeds the permitted use, you will need to obtain permission directly from the copyright holder. To view a copy of this licence, visit <http://creativecommons.org/licenses/by/4.0/>.

References

1. Arge, C.N., Pizzo, V.J.: Improvement in the prediction of solar wind conditions using near-real time solar magnetic field updates. *J. Geophys. Res.* **105**, 10465 (2000). <https://doi.org/10.1029/1999JA000262>
2. Arnaud, J., Newkirk, G.J.: Mean properties of the polarization of the Fe XIII 10747 Å coronal emission line. *A & A* **178**, 263 (1987)
3. Casini, R. and Judge, P.G.: Spectral lines for polarization measurements of the coronal magnetic field. II. consistent treatment of the stokes vector formagnetic-dipole transitions. *AjJ*, **522**, 524. <https://doi.org/10.1086/307629> (1999)
4. Coates, A., Jaumann, R., Griffiths, A., et al.: The PanCam Instrument for the ExoMars Rover. *Astrobiology* **17**, 511 (2017). <https://doi.org/10.1089/ast.2016.1548>
5. Cranmer, S.R., Matthaeus, W.H., Breech, B.A., Kasper, J.C.: Empirical constraints on proton and electron heating in the fast solar wind. *ApJ* **702**, 1604 (2009). <https://doi.org/10.1088/0004-637X/702/2/1604>
6. Cranmer, S.R., van Ballegooijen, A.A., Edgar, R.J.: Self-consistent coronal heating and solar wind acceleration from anisotropic magnetohydrodynamic turbulence. *ApJS* **171**, 520 (2007). <https://doi.org/10.1086/518001>
7. De Moortel, I., McIntosh, S.W., Threlfall, J., Bethge, C., Liu, J.: Potential Evidence for the Onset of Alfvénic Turbulence in Trans-equatorial Coronal Loops. *ApJL* **782**, L34 (2014). <https://doi.org/10.1088/2041-8205/782/2/L34>
8. Eastwood, J.P., Biffis, E., Hapgood, M.A., et al.: The economic impact of space weather: where do we stand? *Risk Anal.* **37**, 206 (2017). <https://doi.org/10.1111/risa.12765>

9. Evans, R.M., Opher, M., Jatenco-Pereira, V., Gombosi, T.I.: Surface Alfvén wave damping in a three-dimensional simulation of the solar wind. *ApJ* **703**, 179 (2009). <https://doi.org/10.1088/0004-637X/703/1/179>
10. Harvey, J. W.: PhD thesis, National Solar Observatory (1969)
11. Keil, S., Oschmann, Jacobus M. J., Rimmele, T. R., et al.: Advanced Technology Solar Telescope: conceptual design and status. In: Oschmann, J., Jacobus, M. (eds.) Society of Photo-Optical Instrumentation Engineers (SPIE) Conference Series, Vol. 5489, Ground-based Telescopes, pp. 625–637. <https://doi.org/10.1117/12.552405> (2004)
12. Kramar, M., Inhester, B., Lin, H., Davila, J.: Vector tomography for the coronal magnetic field II. hanle effect measurements. *ApJ* **775**, 25 (2013). <https://doi.org/10.1088/0004-637X/775/1/25>
13. Lagg, A., Lites, B., Harvey, J., Gosain, S., Centeno, R.: Measurements of photospheric and chromospheric magnetic fields. *SSRv* **210**, 37 (2017). <https://doi.org/10.1007/s11214-015-0219-y>
14. Lavraud, B., Liu, Y. D., Harrison, R. A., et al.: Instant: An Innovative L5 Small Mission Concept for Coordinated Science with Solar Orbiter and Solar Probe Plus. In: AGU Fall Meeting Abstracts, Vol. 2014, SH21B–4109 (2014)
15. Lin, H.: mxSPEC: a massively multiplexed full-disk spectroheliograph for solar physics research. In: Society of Photo-Optical Instrumentation Engineers (SPIE) Conference Series, Vol. 9147, Ground-based and Airborne Instrumentation for Astronomy V, 914712 (2014). <https://doi.org/10.1117/12.2057120>
16. Lin, H.: mxCSM: A 100-slit, 6-wavelength wide-field coronal spectropolarimeter for the study of the dynamics and the magnetic fields of the solar corona. *Front. Astron. Space Sci.* **3**, 9 (2016). <https://doi.org/10.3389/fspas.2016.00009>
17. Lin, H., Casini, R.: A classical theory of coronal emission line polarization. *ApJ* **542**, 528 (2000). <https://doi.org/10.1086/309499>
18. Lin, H., Kuhn, J.R., Coulter, R.: Coronal magnetic field measurements. *ApJL* **613**, L177 (2004). <https://doi.org/10.1086/425217>
19. Lin, H., Penn, M.J., Tomczyk, S.: A new precise measurement of the coronal magnetic field strength. *ApJL* **541**, L83 (2000). <https://doi.org/10.1086/312900>
20. McIntosh, S.W., de Pontieu, B., Carlsson, M., et al.: Alfvénic waves with sufficient energy to power the quiet solar corona and fast solar wind. *Nature* **475**, 477 (2011). <https://doi.org/10.1038/nature10235>
21. Mickey, D.L.: Polarization measurements in the green coronal line. *ApJL* **181**, L19 (1973). <https://doi.org/10.1086/181175>
22. Mikić, Z., & Linker, J. A.: The large-scale structure of the solar corona and inner heliosphere. In: Winterhalter, D., Gosling, J. T., Habbal, S. R., Kurth, W. S., Neugebauer, M. (eds) American Institute of Physics Conference Series, Vol. 382, Proceedings of the eighth International solar wind Conference: Solar wind eight, pp. 104–107 (1996). <https://doi.org/10.1063/1.51370>
23. Morton, R.J., Tomczyk, S., Pinto, R.: Investigating Alfvénic wave propagation in coronal open-field regions. *Nat. Commun.* **6**, 7813 (2015). <https://doi.org/10.1038/ncomms8813>
24. Morton, R. J., Tomczyk, S., & Pinto, R. F.: A global view of velocity fluctuations in the corona below 1.3 R_☉ with CoMP. *ApJ* **828**, 89 (2016). <https://doi.org/10.3847/0004-637X/828/2/89>
25. Ofman, L.: Wave modeling of the solar wind. *Living Reviews in Solar Physics* **7**, 4 (2010). <https://doi.org/10.12942/lrsp-2010-4>
26. Querfeld, C.W., Smartt, R.N.: Comparison of coronal emission line structure and polarization. *SoPh* **91**, 299 (1984). <https://doi.org/10.1007/BF00146301>
27. Shibata, K.: Evidence of magnetic reconnection in solar flares and a unified model of flares. *Ap & SS* **264**, 129 (1999). <https://doi.org/10.1023/A:1002413214356>
28. Sodnik, Z., Heese, C., Arapoglou, P.-D., et al.: Deep-space Optical Communication System (DOCS) for ESA's Space Weather mission to Lagrange orbit L5. In: 2017 IEEE International Conference on Space Optical Systems and Applications (ICSOS), pp. 28–33. (2017) <https://doi.org/10.1109/ICSOS.2017.8357207>
29. Sun, X., Bobra, M.G., Hoeksema, J.T., et al.: Why is the great solar active region 12192 flare-rich but CME-poor? *ApJL* **804**, L28 (2015). <https://doi.org/10.1088/2041-8205/804/2/L28>
30. Suzuki, T. K., & Inutsuka, S.-I.: Making the corona and the fast solar wind: a self-consistent simulation for the low-frequency alfvén waves from the photosphere to 0.3 AU. *ApJL* **632**, L49 (2005) <https://doi.org/10.1086/497536>

31. Thurgood, J.O., Morton, R.J., McLaughlin, J.A.: First direct measurements of transverse waves in solar polar plumes using SDO/AIA. *ApJL* **790**, L2 (2014). <https://doi.org/10.1088/2041-8205/790/1/L2>
32. Tomczyk, S., McIntosh, S.W.: Time-distance seismology of the solar corona with CoMP. *ApJ* **697**, 1384 (2009). <https://doi.org/10.1088/0004-637X/697/2/1384>
33. Tomczyk, S., McIntosh, S.W., Keil, S.L., et al.: Alfvén waves in the solar corona. *Science* **317**, 1192 (2007). <https://doi.org/10.1126/science.1143304>
34. Tomczyk, S., Card, G.L., Darnell, T., et al.: An instrument to measure coronal emission line polarization. *SoPh* **247**, 411 (2008). <https://doi.org/10.1007/s11207-007-9103-6>
35. Tomczyk, S., Landi, E., Burkepile, J.T., et al.: Scientific objectives and capabilities of the Coronal Solar Magnetism Observatory. *J. Geophys. Res. (Space Physics)* **121**, 7470 (2016). <https://doi.org/10.1002/2016JA022871>
36. Uysal, M., & Nouri, H.: Optical wireless communications – An emerging technology. In: 2014 16th International Conference on Transparent Optical Networks (ICTON), pp. 1–7. (2014) <https://doi.org/10.1109/ICTON.2014.6876267>
37. Verth, G., Terradas, J., Goossens, M.: Observational evidence of resonantly damped propagating kink waves in the solar corona. *ApJL* **718**, L102 (2010). <https://doi.org/10.1088/2041-8205/718/2/L102>
38. Wang, Y.M., Sheeley, N.R.J.: Solar wind speed and coronal flux-tube expansion. *ApJ* **355**, 726 (1990). <https://doi.org/10.1086/168805>
39. Webb, D. F. and Howard, T. A.: Coronal mass ejections: observations. *Living Reviews in Solar Physics* **9**, 3. (2012) <https://doi.org/10.12942/lrsp-2012-3>

Publisher's note Springer Nature remains neutral with regard to jurisdictional claims in published maps and institutional affiliations.